Title: Integrated evolutionary and structural analysis reveals xenobiotics and pathogens as the major drivers of mammalian adaptation

Greg Slodkowicz[1,2,3*] and Nick Goldman[1,4*]

1. European Molecular Biology Laboratory, European Bioinformatics Institute (EMBL-EBI), Wellcome Genome Campus, Hinxton, CB10 1SD, UK

2. Current address: MRC Laboratory of Molecular Biology, Hills Road, Cambridge CB2 0QH, UK

3. gslodko@mrc-lmb.cam.ac.uk

4. goldman@ebi.ac.uk

* Corresponding author

Abstract

Understanding the molecular basis of adaptation to the environment is a central question in evolutionary biology, yet linking detected signatures of positive selection to molecular mechanisms remains challenging. Here we demonstrate that combining sequence-based phylogenetic methods with structural information assists in making such mechanistic interpretations on a genomic scale. Our integrative analysis shows that positively selected sites tend to co-localise on protein structures and that positively selected clusters are found in functionally important regions of proteins, indicating that positive selection can contravene the well-known principle of evolutionary conservation of functionally important regions. This unexpected finding, along with our discovery that positive selection acts on structural clusters, opens new strategies for the development of better models of protein evolution. Remarkably, proteins where we detect the strongest evidence of clustering belong to just two functional groups: components of immune response and metabolic enzymes. This gives a coherent picture of immune response and xenobiotic metabolism as the drivers of adaptive evolution of mammals.

Introduction

Over the course of evolution, the genomes of all organisms are shaped by the environment. The results of this process can be observed by comparing evolutionarily related sequences from different species: regions that code for essential cellular functions can remain unaltered over hundreds of millions of years, while changing evolutionary pressures can lead to emergence of new functions over very short evolutionary timescales. As a result, evolutionary histories of sites in the genome hold information about their functional importance. Functionally important regions are routinely identified by taking advantage of the fact that they are highly conserved in evolution [1,2]. Similarly, methods for detecting regions harbouring adaptive changes have been developed to take advantage of the fact that rapid fixation of new alleles is a hallmark of positive selection [3,4]. Analyses of patterns of evolutionary change can identify specific cases of adaptation as well as reveal general principles that guide evolution [5]. Understanding evolutionary processes and distinguishing between neutral and adaptive changes is therefore one of the key aims of modern evolutionary studies.

As most proteins have to maintain a specific three-dimensional shape to perform their function, protein-coding genes exhibit particularly complex patterns of substitution. Biophysical constraints restrict the allowed amino-acid substitutions and result in dependencies across the entire protein sequence. While structural features can explain a significant proportion of observed site-to-site rate variation [6], previous studies have focused on evolutionary scenarios where existing functions are maintained and little is known about the structural properties of sites evolving under positive selection.

Present lack of understanding of structural aspects of adaptive evolution is particularly surprising bearing in mind that many single-gene studies took advantage of protein structure to assess the functional significance of positively selected sites identified from sequence data. In the classic study of Hughes and Nei [7], positively selected residues in the MHC molecule were found to cluster in the groove where pathogen-derived peptides are bound, supporting

70 the hypothesis that rapid amino-acid substitutions at these sites tuned the ability to bind
71 peptides derived from pathogens. Similarly, positively selected sites in TRIM5α, a viral
72 restriction factor that can inhibit the cellular entry of HIV in non-human primates, are placed in
73 the region that mediates binding to the virus [8]. In these studies, as in others (e.g. [9]), proximity
74 of positively selected residues on the protein structure was used as corroborating evidence
75 and helped assign a molecular mechanism underlying detected adaptations.

76 As the amount of available genomic data increased, studies of positive selection in individual
77 proteins were followed by genome-wide positive selection scans [10-15]. Such genomic scans,
78 using appropriately adapted statistical methodology [16,17], can identify which cellular processes
79 are primary targets of positive selection and generate testable hypotheses. However,
80 structural aspects of identified examples were largely neglected and so no coherent view of
81 how protein structure affects adaptive evolution has emerged from these investigations.

82 This is a significant gap in our understanding of evolution. Biophysical constraints restrict what
83 substitutions are allowed for protein function to be maintained and are also likely to limit the
84 emergence of adaptive changes in response to pressures from the environment, yet no
85 evolutionary theory predicts the structural properties of sites harbouring adaptive changes. It
86 is not established whether positive selection is more likely to act on protein sites where the
87 effect of mutations is the largest (e.g. enzyme catalytic sites or key interaction interfaces) or
88 regions where mutations likely have a smaller effect (e.g. allosteric regulation sites). Adaptive
89 changes are associated with rapid fixation of advantageous mutations, yet functional regions
90 are thought to be highly conserved in evolution. Contrasting these two principles leads to an
91 apparent paradox.

92 Here, we integrated structural information into evolutionary analyses in order to study the
93 properties of positively selected sites. We demonstrate that detailed mechanistic interpretation
94 of findings can be achieved on a genome-wide level, just as in the case of earlier studies of
95 individual proteins. In recent years, it has become apparent that structural data can be an

96 orthogonal source of information that can serve to validate and augment findings in different
97 areas of genomics [18]. Structural placement of sites of interest, such as those identified through
98 genome-wide sequence analyses, can be used to strengthen the confidence in findings —
99 clustering of sites indicates concerted function whereas unrelated sites are expected to be
100 more uniformly distributed in the structure. Recently developed methods based on clustering
101 of sites on protein structures have been successful in distinguishing causal and hitchhiking
102 mutations underlying genetic diseases [19] and for identifying mutations with functional impact
103 in cancer [20-23]. Detailed information about the protein structure can similarly aid understanding
104 of molecular mechanisms underlying adaptation at detected sites.

105 To obtain a structurally-informed view of positive selection at the residue level, we developed
106 an approach combining a genome-wide scan for positive selection with structural information
107 (fig. 1a). We applied 3D clustering to detect genes with positively selected sites in a robust
108 manner that additionally allowed us to link identified cases to an underlying molecular
109 mechanism. We demonstrate that positively selected sites tend to occur close to one another
110 on protein structure and detect 20 high-confidence positively selected clusters (table 1).
111 Strikingly, we find that all but one of the identified cases are immune-related proteins or
112 metabolic enzymes. In both of these functional categories, interactions with dynamic
113 environmental parameters appear to have shaped the evolutionary histories of the genes
114 involved. By further analysing the placement of positively selected clusters, we find that
115 pervasive positive selection acts on regions that are typically highly conserved in evolution,
116 suggesting new strategies for the development of more accurate models of protein evolution
117 and methods for detecting positive selection.

118

119

120

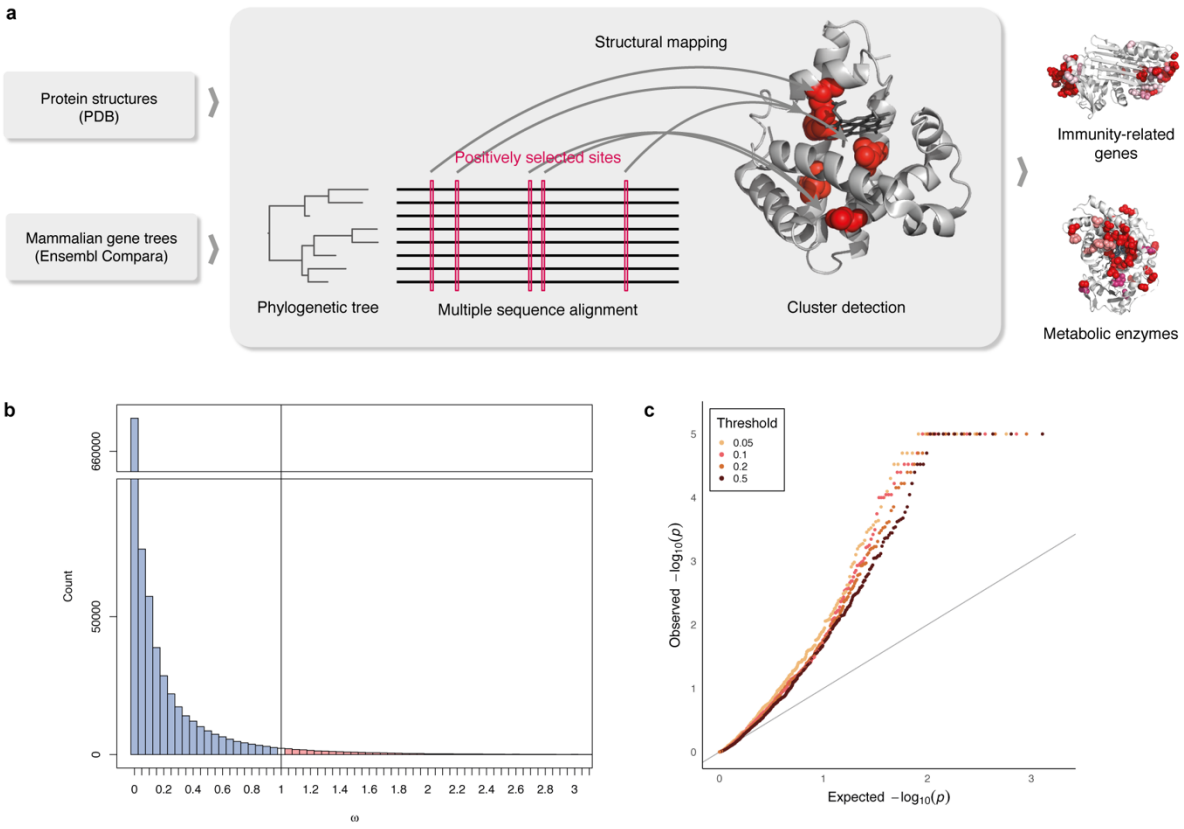

Figure 1. Positively selected residues tend to cluster together (a) Overview of the approach (b) Distribution of ω values in the dataset. With 97.6% of sites having $\omega < 1$ (indicating purifying selection), and 2.4% with $\omega \geq 1$, the mean of ω across the entire dataset is 0.126. (c) QQ plot of *p*-value distribution obtained from CLUMPS applied to positively selected sites at FDR of 0.05, 0.1, 0.2 and 0.5. If the residues under positive selection were randomly distributed on protein structures, we would expect a uniform distribution of *p*-values (grey line). The observed *p*-values are lower than would be expected under the null hypothesis of random placement, indicating that positively selected sites tend to cluster together.

Results

Identification of positive selection. In order to identify residues that were under positive selection in mammalian evolution, we obtained coding sequences for Eutherian mammals from Ensembl and phylogenetic trees from the Ensembl Compara database [24]. 3D structures corresponding to human proteins in our dataset were then downloaded from PDB [25] and

136 mapped against protein sequences using the SIFTS resource [26]. We aligned coding
137 sequences corresponding to each tree using the PRANK aligner [27] and used the Slr software
138 [28] to detect positively selected sites. The resulting dataset comprises 3,347 protein alignments
139 and covers 1,021,133 structure-mapped amino-acid sites. While the majority of sites evolve
140 under purifying selection (fig. 1b), consistent with both theoretical expectations and previous
141 empirical estimates [13], we identified 4,498 sites with strong evidence of positive selection
142 (FDR=0.05). We have made these results available as an online resource which allows for
143 displaying and downloading of the structure-mapped sitewise estimates of selective
144 constraint, as well as the underlying alignments and phylogenetic trees
145 (http://wwwdev.ebi.ac.uk/goldman-srv/slr/).

146 **Detecting clustering of positively selected sites.** To determine the degree of clustering of
147 positively selected sites, we applied a modification of the CLUMPS algorithm [21] to our
148 integrated dataset (see Methods). As the power to detect clustering is limited if very few
149 residues are considered, it is desirable to include as many sites with evidence of positive
150 selection as possible. At the same time, reducing the stringency in the detection of selection
151 by allowing a higher false discovery rate (FDR) can dilute the signal of clustering by including
152 more false positives. As it is not clear *a priori* what the tradeoff between these phenomena is
153 and at what threshold the power to detect clustering is maximised, we applied the chosen
154 clustering detection method separately to positively selected sites detected at different
155 stringency levels. In order to determine the degree to which positively-selected residues form
156 clusters on protein structures, we inspected the overall distribution of *p*-values obtained for
157 each protein from CLUMPS at four FDR thresholds at which positively selected sites were
158 detected (fig. 1c). We find a significant tendency for positively selected sites to cluster together
159 and this trend is maintained at each FDR threshold, indicating that our findings are robust to
160 how stringently positively selected sites are identified.

161 **Clusters of positively selected sites** Having established that positively selected sites tend
162 to occur close to one another on protein structures, we went on to select cases where evidence
163 for clustering is the strongest. Depending on the FDR threshold used to identify sites as
164 positively selected, between 35 and 52 proteins with clusters of positively selected residues
165 were detected (FDR of clustering <0.05), with substantial overlap between clusters detected
166 at different thresholds (suppl. fig. 2). For 22 proteins, clusters were identified at all four FDR
167 thresholds suggesting that these constitute the most robust findings. For these proteins, we
168 inspected the underlying alignments from which positively selected sites were identified.
169 Correlation on the sequence level can introduce clusters on the level of structure and for this
170 reason it is important to distinguish 3D clusters resulting purely from closeness of sites of
171 interest in the sequence. In all but two cases, we find that positively selected sites are identified
172 in regions of good alignment quality and that clusters of positively selected sites arise mostly
173 from residues that are not adjacent in the sequence and become close to each other only
174 once the protein is folded into its native conformation. The two cases where detected signature
175 of positive selection appears to result from a stretch of contiguous residues in a region of poor
176 alignment quality were rejected from further analysis. The remaining 20 proteins are
177 summarised in table 1. Remarkably, nine of them are immune-related proteins and ten are
178 metabolic enzymes. The remaining protein, nicastrin, is the substrate-recruiting component of
179 gamma-secretase [29], a protein complex with catalytic activity and we therefore consider it
180 together with other enzymes.

181 **Positive selection in proteins involved in immunity**

182 **Confirmation of validity of clustering approach** Rapid evolutionary rates in genes involved
183 in both adaptive and innate branches of the immune system are a classic example of positive
184 selection [7,8,30-32]. Proteins where we identified positively-selected clusters (table 1) include
185 cases where positive selection has been documented previously, such as in HLA-DRB1 [7],
186 CD1a [33], TLR4 [33] and TfR, a protein which is known to have been hijacked by arenaviruses

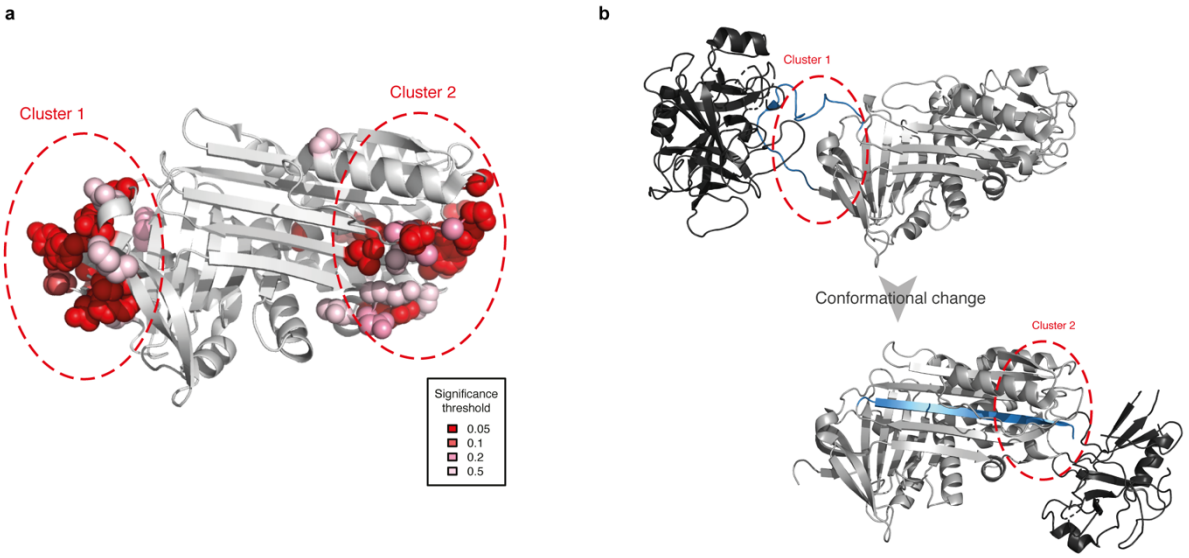

187

188 **Figure 2. Clusters of positively selected sites in serpin B3** (a) Placement of positively selected sites
189 on the structure of serpin B3 (PDB 4zk0). (b) Mode of action of serpins shown using PDB structures
190 1k9o (top) and 1ezx (bottom) with the substrate shown in black and the RCL marked in blue. Regions
191 analogous to those where positively selected clusters were marked as in (a). Serpins function by binding
192 their target proteases using a reactive center loop (RCL) that mimics the protease substrate. They then
193 form a covalent bond with the protease and undergo a large conformational change resulting in the
194 protease being deformed and then acylated [35,36]. We find that positively selected residues surround the
195 RCL and are also located on the opposite side of the protein to which the bound protease is dragged.

196

197 for facilitating cellular entry [34]. Positively selected residues are located primarily in regions
198 involved in antigen binding, such as the structurally similar binding clefts of HLA-DRB1 and
199 CD1a (suppl. fig. 3-6). While these findings were reported previously, they give confidence in
200 the approach we applied here.

201 **Novel findings of selection clusters** We also identify cases where to our knowledge positive
202 selection has not been previously described: ficolin 2 (suppl. fig. 7; though positive selection
203 in the related ficolin-3 has been reported [37]), complement component 5 (suppl. fig. 8),
204 complement component 8α (suppl. fig. 9), SIGLEC5 (suppl. fig. 10) and serpin B3 (fig. 2).

205 The placement of positively selected sites in serpin B3 is particularly interesting as this protein
206 exhibits two clusters concentrated on the opposite poles of the protein (fig. 2a). Serpin B3
207 belongs to the serpin superfamily of protease inhibitors, though unlike most serpins it binds
208 cysteine rather than serine proteases. Serpins contribute to immunity by inhibiting proteases
209 secreted by bacteria. Serpin B3 inactivates leaked lysosomal cathepsins, inactivates
210 pathogen-derived cathepsins and is also thought to be involved in autoimmunity [38].
211 Comparison with other available structures of serpins reveals a remarkable correspondence
212 of these positively selected sites to the protease binding sites before and after the
213 conformational change that characterises the mode of action of serpins (fig. 2b). Furthermore,
214 there is previous evidence that serpin B3 homologs have changed their substrate specificities
215 over the course of evolution consistent with the action of positive selection [39,40]. The presence
216 of two positively selected residue clusters at opposite poles of the protein implies that both
217 regions participate in the tuning of function. The importance of these regions in the proteolytic
218 function of serpins demonstrates that the positive selection we detect is likely to have
219 functional consequences.

220 Interactions with pathogens are known to be one of the dominant pressures shaping
221 mammalian evolution [30]. Our analysis adds mechanistic details to these findings: positively
222 selected clusters in proteins involved in host-pathogen interactions are placed in regions
223 directly mediating binding of pathogen-derived molecules. Binding of pathogen-derived
224 peptides by HLA and subsequent triggering of the immune response is a classic example of
225 this [41]. Here we have identified further examples of similar mechanisms in components of both
226 innate and adaptive branches of the immune system. Interestingly, these include not only
227 proteins or protein-derived peptides but also lipids (CD1a) and lipopolysaccharides (TLR4).
228 This is true both when binding is facilitating the neutralisation of pathogens and, as in the case
229 of TfR, where host proteins are hijacked by a pathogen to facilitate cellular entry. These
230 scenarios are examples of high evolutionary rate being the result of an ‘arms race’ between

host and pathogen. Such dynamics are predicted by the Red Queen hypothesis, which posits that evolution is driven by inter-species competition [42].

Positive selection acting on metabolic enzymes

Cytochrome P450s Ten out of eleven remaining positively selected clusters are found in enzymes. Three of the identified clusters of positively selected sites are in members of the cytochrome P450 (CYP) superfamily (fig. 3). CYPs are the most important drug-metabolising enzyme class, contributing to the metabolism of 90% of drugs as well as many other xenobiotics such as pollutants. These liver enzymes catalyse monooxygenation reactions on a wide range of small and large substrates. More than 50 CYPs have been identified in the human genome but relatively few are known to have a role in drug metabolism [43].

Strikingly, all three of the CYPs where we identify positively selected clusters of residues are known to be important for drug metabolism: CYP3A4 (fig. 3a-b) is the most promiscuous of all CYPs, contributing to the metabolism of ~50% of marketed drugs, and CYP2C9 (fig. 3c-d) and CYP2D6 (fig.3e-f) are also among the six principal CYPs thought to contribute the most to drug metabolism [44]. In our dataset, alignments containing the three CYPs mentioned before also contain two further cytochrome P450 paralogs that are important for drug metabolism — in total 5 out of 6 enzymes thought to be responsible for the majority of cytochrome P450 drug metabolism show evidence of positive selection.

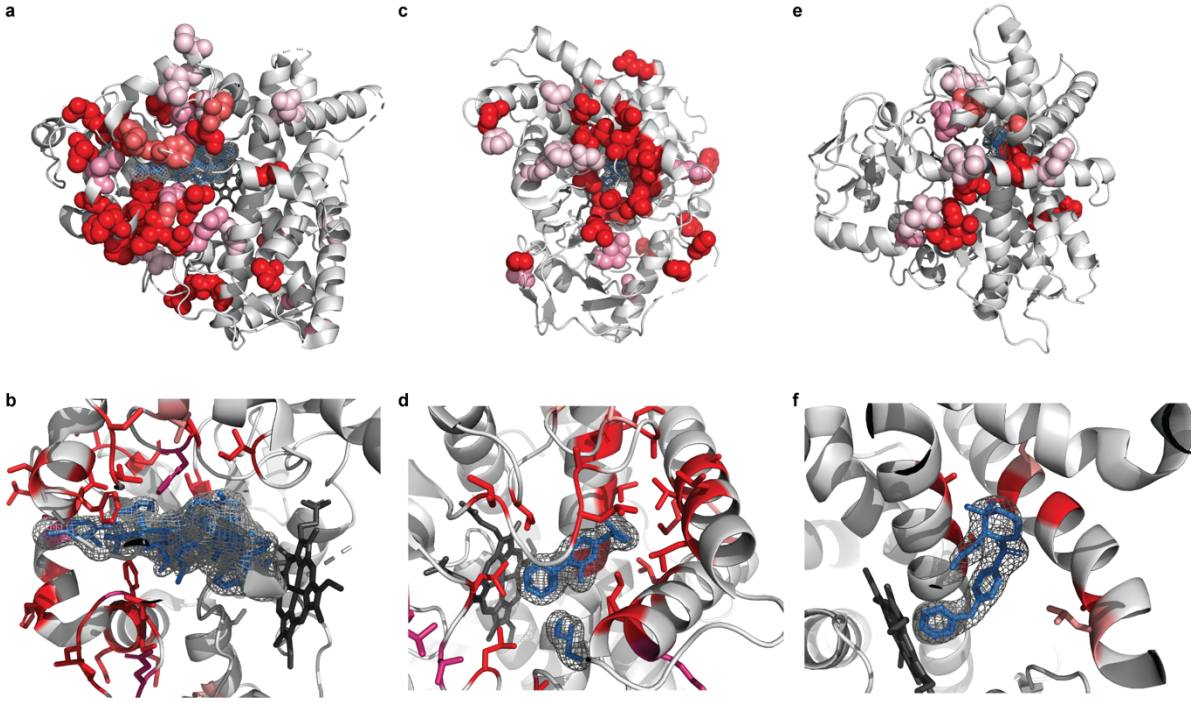

Figure 3. Positively selected residues in CYPs cluster in the substrate entry channel and catalytic site Positively selected residues in (a, b) CYP3A4 (PDB 3tjs), (c, d) CYP2C9 (PDB 1r9o) and (e, f) CYP2D6 (PDB 2f9q). Hemes are shown coloured in dark grey, other ligands in blue. Additional ligands were transferred from other PDB structures by superimposition: (a, b) desthiazolylmethyloxycarbonyl ritonavir, ketoconazole (PDB 2v0m), erythromycin (PDB 2j0d). (c, d): flurbiprofen (e, f) prinomastat (PDB: 3qm4). Specificity for the extraordinary diversity of substrates in this enzyme superfamily is facilitated by a large, flexible binding pocket at the bottom of which heme is located. In all three structures, the location of the positively selected residues tracks the binding of a ligand, and in general can be found on the sides of helices and in loops that form the binding pocket.

Aldo-keto reductases We identified positively-selected clusters in two members of the 15 aldo-keto reductases (AKRs) present in human. Similarly to CYPs, AKRs are a family of highly promiscuous enzymes that utilise NAD(P)(H) co-factors and can reduce a wide range of substrates [45]. AKRs are part of phase II metabolism and can transform or detoxify both endogenous and environmental aldehydes and ketones [46-48]. Positively selected residues in both AKRs cluster around the region where the substrate binds but not around the NADP+ co-

266 factor (fig.4). This suggests that evolution has tuned substrate specificity while maintaining
267 binding to the cofactor.

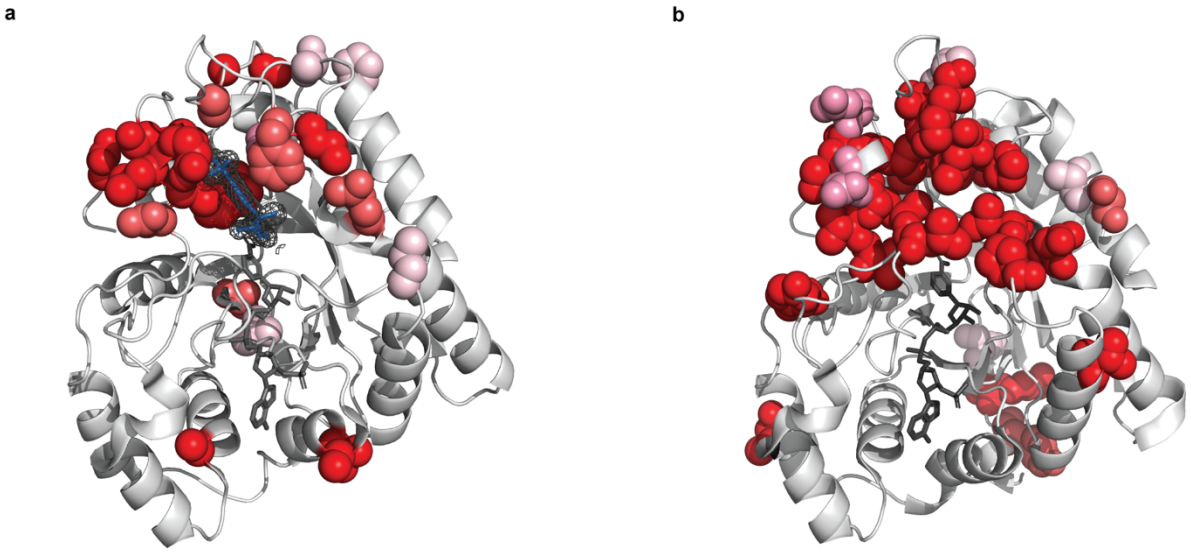

268

269 **Figure 4. Positively selected residues in AKRs surround the substrate binding site** positively
270 selected residues in (a) AKR1B10 (PDB 1zua) and (b) AKR1C4 (PDB 2fvl). Tolrestat marked in blue,
271 NADP+ marked in dark grey. Positively selected residues in AKR1B10 cluster around the bound ligand
272 tolrestat, an inhibitor developed for diabetes treatment, but not around the NADP+ cofactor. The
273 structure of AKR1C4 has been solved without ligand but the positively selected residues cluster in a
274 similar region of the structure when compared to AKR1B10. As in the case of AKR1B10, there are no
275 positively selected residues in the neighbourhood of the NADP+ cofactor.

276

277 **Other enzymes** We also identified individual positively selected clusters in the members of
278 three other protein families involved in detoxification: glutathione S-transferase alpha 3 [49-52],
279 carboxylesterase 1 [53,54] and sulfotransferase 2A1 [55,56]. In all cases, positively selected sites
280 cluster around the active site of the enzyme where the substrate binds (fig. 5a-c).

281 In the remaining three cases, positively selected clusters are located in sub-domains that
282 interact with substrates. Adenylate kinase 5 (AK5) is a member of a family of enzymes

283 important for maintaining the energetic balance in the cell by converting ADP into ATP [57].
284 Positively selected residues in AK5 fall in the lid sub-domain (fig. 5d) which has been shown
285 to have a role in tuning the enzyme activity [58]. The three positively selected sites that constitute
286 the positively selected cluster in AK5 flank a DD motif which is highly conserved in AK5 and
287 in other enzymes of the family. Experimentally mutating a residue homologous to V507, one
288 of the sites we have predicted, has been shown to have an effect on the enzyme's kinetic
289 parameters [59], strongly suggesting that the positively selected sites we detect contribute to
290 enzyme specificity and kinetics.

291 In the case of oleoyl-ACP hydrolase (OLAH), an enzyme involved in controlling the distribution
292 of chain lengths of fatty acids, positively selected residues are located in the capping domain
293 that covers the substrate (fig. 5e). Detailed mutational data for OLAH is lacking but enzymes
294 of the same class have been shown to undergo changes of specificity in other species [60].
295 Positively selected sites in nicastrin (suppl. fig. 11) are primarily located in the lid domain that
296 covers the substrate [61], and changes at positively selected sites in these enzymes are
297 therefore also consistent with positive selection acting to fine-tune enzymatic activity.

298 Pervasive positive selection in metabolic enzymes, similar to that experienced by immune-
299 related genes, may seem surprising. Although examples of episodic adaptation of enzymes in
300 specific lineages, particularly in primates, exist [62,63], signatures of pervasive positive selection

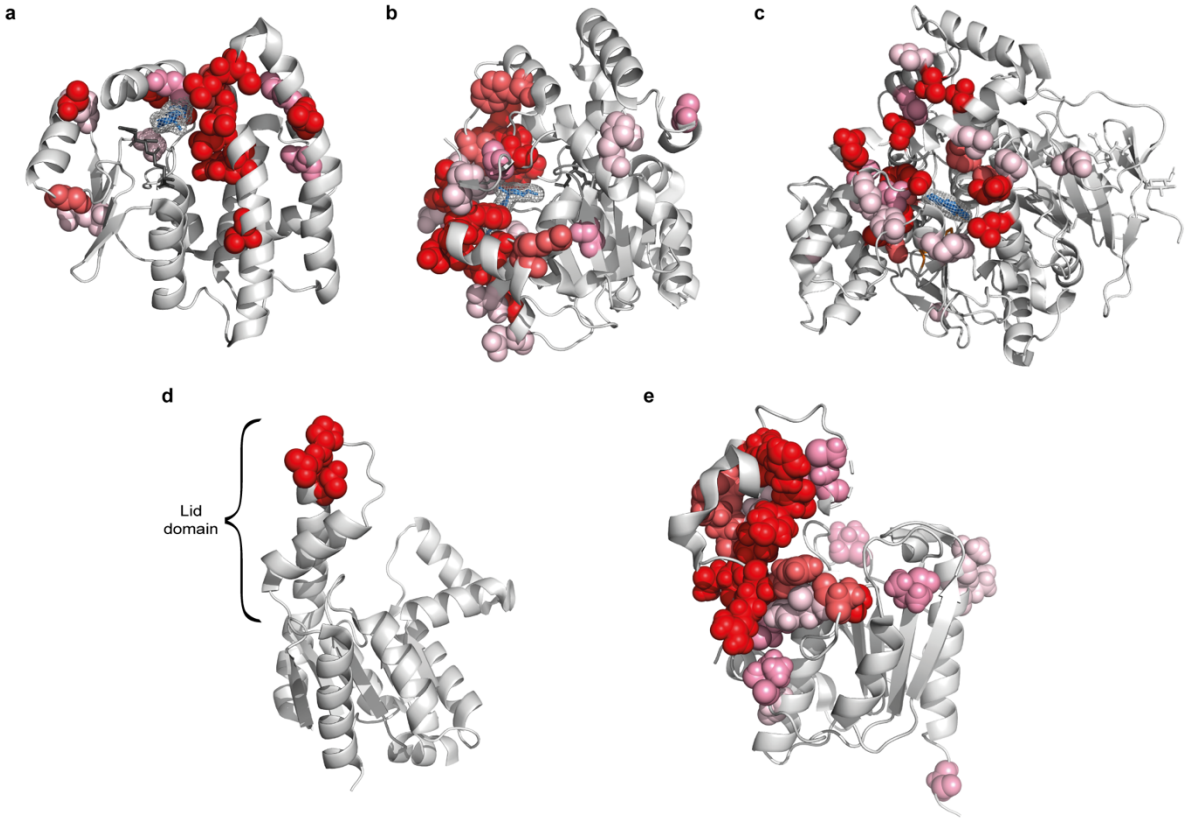

301

302 **Figure 5. Positively selected residues in other enzymes** (a) Positively selected sites in GSTA3 (PDB
303 1tdi). Glutathione shown in dark grey, delta-4-androstene-3-17-dione (blue) transferred by structure
304 superimposition from structure 2VCV. (b) Positively selected residues in sulfotransferase 2A1 (PDB
305 3f3y). Adenosine-3'-5' diphosphate shown in dark grey, lithocholic acid shown in blue. (c) Positively
306 selected sites in carboxylesterase 1 (PDB 1mx1). Tacrine shown in blue. (d) Positively selected residues
307 in adenylate kinase 5 PDB (PDB 2bwj). (e) Positively selected sites in oleoyl-ACP hydrolase (PDB 4xjv).

308

309 were not previously thought to be common in enzymes. However, enzymes where we
310 identified positively selected clusters are involved in interactions with the environment and
311 share a number of other characteristics that make them plausible targets of positive selection.
312 Eight out of ten such enzymes we identified are involved in the catalysis of xenobiotics. Much
313 like parts of the immune system that directly interact with pathogens, these metabolic enzymes
314 form an interface with the environment and act as one line of defence. The diversification of
315 mammals involved adaptation to varied environments and new diets and as the environment

316 in which they live and feed has changed, so did their exposure to toxins. This is likely to have

317 required widespread, repeated adaptive changes that we observe.

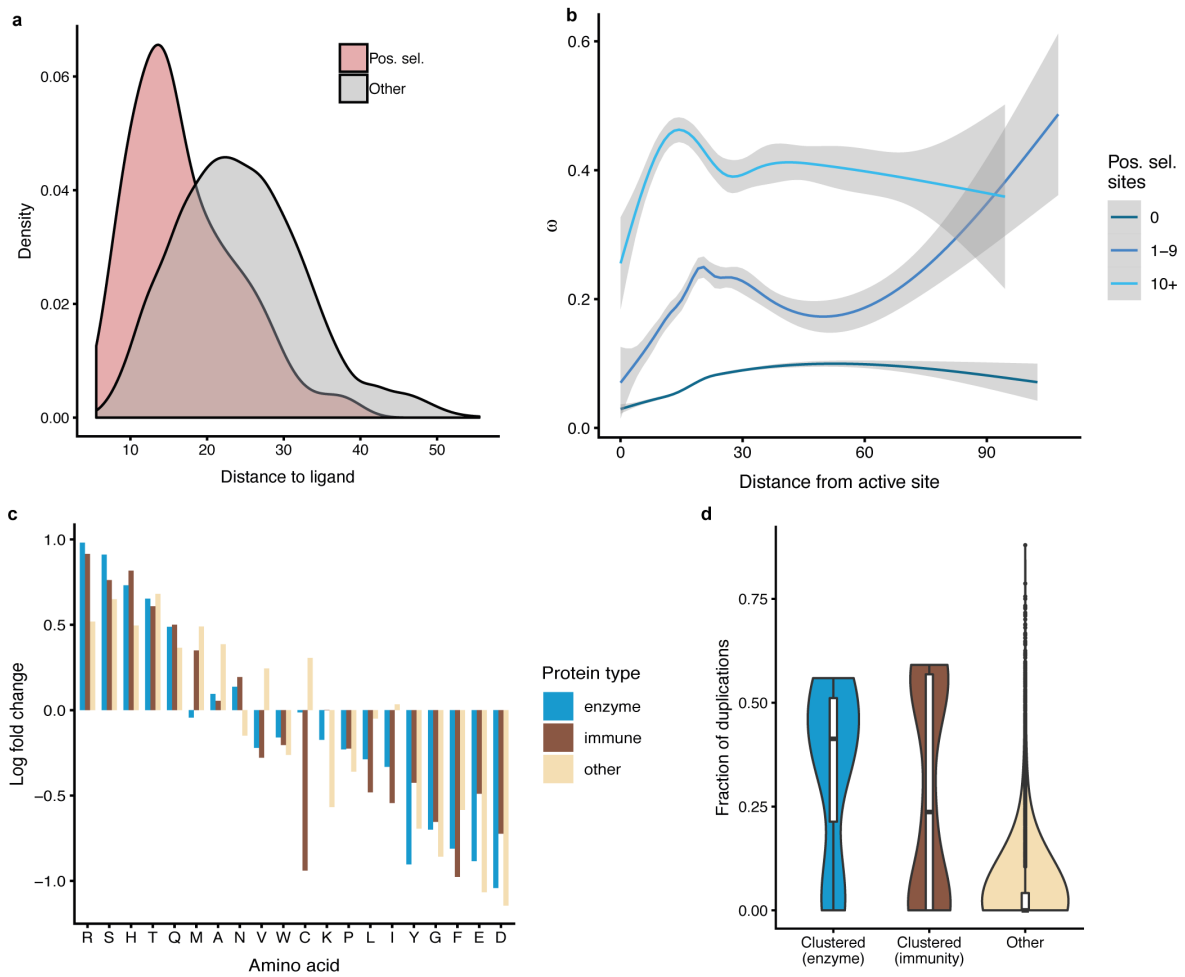

318

319 **Figure 6. Properties of positively selected sites** (a) Distance of positively selected residues from

320 bound exogenous ligands. (b) The distribution of ω as a function of distance from catalytic residues. (c)

321 Departures from the background amino acid frequencies in positively selected residues. (d) Distribution

322 of fraction of gene duplications in proteins with positively selected clusters.

323

324 **Placement of positively-selected sites in relation to functional sites** Having observed the

325 tendency of observed clusters to occur in the direct neighbourhood of bound ligands, we

326 sought to quantify this trend. For structures solved with exogenous ligands, we obtained the

327 distribution of distances for positively-selected residues and compared them to remaining

328 residues (fig. 6a). We find that positively selected residues are significantly closer to those

329

330 ligands (mean distance 16.9Å vs. 24.4Å; $P < 2.2\times10^{-16}$; Kolmogorov-Smirnov test),
331 confirming that positively-selected clusters tend to occur closer to bound ligands than would
332 be expected by chance and providing further evidence for positive selection acting to fine-tune
333 ligand binding.

334 We then investigated the overall distribution of ω as a function of distance to catalytic sites,
335 using annotations from Catalytic Site Atlas [64]. In proteins where we detected no evidence of
336 positive selection, purifying selection is the strongest in the neighbourhood of catalytic sites
337 and gradually relaxes with distance from them (fig. 6b). This trend is consistent with previous
338 studies of selective constraint where positive selection was not considered [65]. However, in
339 cases where we detected positively selected sites we observed a very different distribution of
340 ω, with a peak at 20Å from the catalytic residues. In cases where we detected 10 or more
341 positively selected sites, this trend is even more pronounced, with the peak of ω occurring at
342 14Å from catalytic residues. The enrichment of positively selected residues and elevated
343 mean ω in the neighbourhood of catalytic sites indicates that the action of positive selection
344 reshapes the selective constraint on the entire protein structure.

345 **Properties of amino acids at positively selected sites** As different regions of proteins are
346 known to have different amino-acid frequencies [66,67], we asked whether the positively selected
347 residues we detected exhibit a distinct amino acid distribution. For each protein class, we
348 calculated the change in amino acid frequency at positively selected sites compared to the
349 background frequencies (fig. 6c). While the overall distributions of amino acids are very similar
350 in the different proteins classes (suppl. fig. 12), we observe differences in the distribution of
351 amino acids at positively selected sites compared to the background distribution (fig. 6c). We
352 correlated these enrichment scores with common amino acid physicochemical properties
353 (size, hydrophobicity, net charge and polarity) but found no significant correlations (suppl.

354 table 1), indicating that, while certain amino acids are preferred or avoided at positively
355 selected sites, these trends bear no straightforward relationship to amino acid properties.

356 **The role of gene duplication events in adaptive evolution** Gene duplications are thought
357 to be one of the main forces driving evolution, providing 'raw material' for evolutionary
358 innovations [68]. While gene duplications events in themselves are frequently assumed to have
359 no effect on fitness, their retention can be evidence of adaptation [69]. In order to quantify the
360 effect of duplication events in our dataset, we calculated the fraction of gene duplications (i.e.
361 the number of duplication nodes divided by the total number of nodes) for each phylogenetic
362 tree. We find that both in enzymes and in immune-related genes, the mean paralog fraction is
363 significantly larger than in other genes (0.342 and 0.276, respectively, compared to 0.0397 in
364 the remaining trees; fig. 6d). This trend is significant both in the case of immune proteins and
365 metabolic enzymes ($P = 0.015$ and $P = 3.1\times10^{-5}$, respectively; Kolmogorov-Smirnov test).
366 This elevated duplication rate in genes where we detected positively selected clusters is
367 consistent with positive selection acting not only on point mutations but also driving gene
368 duplication events to fixation. At the same time, some genes where we detected strong
369 evidence of adaptation (complement component 5, transferrin receptor 1, complement
370 component 8α, adenylate kinase 5 and nicastrin) have not undergone any gene duplications,
371 proving that rapid sitewise evolutionary rate and gene duplications can occur independently.

372 **Discussion**

373 In this study, we curated a dataset covering over one million structurally mapped sites in 3,347
374 mammalian proteins and assessed the placement of positively selected residues on their 3D
375 structures in an unbiased, genome-wide manner. We find that positively selected sites tend to
376 occur closer to each other in protein structures than is expected by chance and to form clusters
377 in the neighbourhood of functionally important regions. Strikingly, proteins where we found the
378 strongest evidence for clustering of positively selected sites are primarily involved in two major
379 types of environmental responses: host-pathogen interactions and metabolism of xenobiotic

380 compounds. The fact that we observe the strongest evidence of positive selection in these
381 types of proteins gives a coherent view of mammalian evolution being shaped by these two
382 major influences from the environment. Clusters of positively selected sites we identified share
383 both functional and structural similarities and allow us to infer more general principles
384 underlying adaptive evolution.

385 Xenobiotic-metabolising enzymes are typically able to process a wide range of substrates.
386 Indeed, CYPs and AKRs, where we identified three and two positively selected clusters,
387 respectively, are among the most promiscuous known protein superfamilies. Promiscuous
388 enzymes are thought to be malleable in evolution, as they can maintain their original function
389 as well as acquire specificity for new substrates by going through a promiscuous intermediate
390 which can bind multiple substrates [70]. The mechanisms by which enzymes acquire new
391 substrates has to date been primarily studied by directed evolution [71-74]. The examples we
392 have highlighted here provide direct evidence that similar scenarios are also common in
393 natural evolution.

394 Enzymes involved in xenobiotic metabolism are of great medical relevance, as in humans they
395 are responsible for metabolism of prescribed drugs. Traditional analyses of protein
396 conservation are frequently not suitable for the analysis of genes involved in xenobiotic
397 metabolism, as these tend to evolve rapidly and the analyses used do not explicitly distinguish
398 between neutral evolution and positive selection [75]. Specific examples we have identified here
399 could be investigated further, for example by detailed mutational studies that have been shown
400 to augment statistical modelling of adaptive evolution [76].

401 Our study highlights the power of incorporating independent sources of information to
402 understand principles governing evolution. The clusters we detected consist of residues that
403 are distributed along the linear sequence of proteins and could not be found without
404 considering protein structure. Consideration of structural information has also allowed us to
405 better understand the mechanistic details of processes underlying adaptation in terms of

406 specific structural and functional features. Information about structural placement of residues
407 can also help to address technical issues that have hindered methods for detecting positive
408 selection. Criticisms levelled at methods for detecting positive selection have revolved around
409 the non-neutrality of synonymous substitutions, local variation in synonymous substitution rate
410 [77-80] and the influence of errors in alignment [81,82]. These phenomena may cause false positives
411 in parts of a protein sequence, but none will result in clustering on protein structure. Structural
412 information can thus serve as an independent validation and a means of demonstrating that
413 observed patterns of positive selection are not a product of confounding factors. Structural
414 clusters can additionally be inspected *post hoc* for proximity to functional features to assess
415 their plausibility and aid interpretation.

416 The structural and functional similarities we identified here point towards common rules
417 governing the occurrence of pervasive positive selection. Positively selected metabolic
418 enzymes we described here share many structural and functional similarities: positively
419 selected clusters lie in close proximity to bound ligands, indicating that the primary mode in
420 which these enzymes adapt is by affecting residues in the direct neighbourhood of active sites.
421 This finding may seem to contradict the common assumption that functionally important
422 residues are conserved in evolution: for example, the finding that average evolutionary rate is
423 lowest in the neighbourhood of catalytic sites [65]. However, this is only a superficial
424 disagreement: while functional regions evolve more slowly on average, this does not mean
425 that cannot harbour rapidly evolving, positively selected sites. Indeed, non-functional regions
426 cannot, by definition, undergo adaptive evolution.

427 As we demonstrate here, while functional regions of proteins are typically more conserved,
428 they can also exhibit a high evolutionary rate that is a hallmark of adaptive evolution. This
429 strongly suggests that instances where positive selection is operating can contradict overall
430 trends of protein evolution. For this reason, it may be counterproductive to incorporate known
431 correlates of evolutionary rate into statistical models for detecting positive selection. In

432 contrast, the fact that positively selected residues can form clusters on protein structures could
433 inform the development of better methods for detecting positive selection. One of the ultimate
434 goals of evolutionary research is integrating evolution of sequence with structure in a general
435 model of protein evolution [83,84]. Such a universal model of protein evolution has been elusive
436 so far, primarily because the most general approaches require an intractable number of
437 parameters. We would suggest that one way forward is to identify further universal
438 evolutionary trends and gradually incorporate them into mathematical models of protein
439 evolution.

440 We have demonstrated that analysing selective constraint in the context of structure can help
441 interpret findings and increase their robustness, but all approaches reliant on detailed
442 structural information are limited by the availability and coverage of crystal structures. We
443 hope that the results highlighted here and others we made available online in our web server
444 will assist experimental validation and further understanding of protein function and
445 adaptation. We aimed to establish the relationship between protein structure and the
446 occurrence of positive selection and this proof-of-principle study called for the highest-possible
447 quality data, but incorporating homology-based structural models would be a direct extension
448 to our approach. It is likely that the PDB database is currently biased towards certain protein
449 families which suggests that in future more examples of adaptation will be identified in protein
450 families where currently little or no structural information is available. Similarly, the analysis
451 performed here focused on mammals but could be extended to other clades.

452 **Acknowledgements**

453 We would like to thank Dr Leo C. James, Dr M. Madan Babu, Dr Patrycja Kozik, Dr Maria
454 Marti-Solano and members of the Goldman Group at EMBL-EBI for helpful discussions and
455 comments on the manuscript.

456

457 **Author Contributions**

458 G.S and N.G. conceived the study. G.S. performed all analyses. N.G. supervised the research.

459 G.S. and N.G. wrote the manuscript.

460 **Competing interests**

461 The authors declare no competing interests.

References

1. Havrilla, J.M., Pedersen, B.S., Layer, R.M. & Quinlan, A.R. A map of constrained coding regions in the human genome. *Nat Genet* **51**, 88-95 (2019).
2. Fuller, Z.L., Berg, J.J., Mostafavi, H., Sella, G. & Przeworski, M. Measuring intolerance to mutation in human genetics. *Nat Genet* **51**, 772-776 (2019).
3. Yang, Z. PAML 4: phylogenetic analysis by maximum likelihood. *Mol Biol Evol* **24**, 1586-91 (2007).
4. Weaver, S. *et al.* Datamonkey 2.0: a modern web application for characterizing selective and other evolutionary processes. *Mol Biol Evol* (2018).
5. Benner, S.A. Natural progression. *Nature* **409**, 459 (2001).
6. Echave, J., Spielman, S.J. & Wilke, C.O. Causes of evolutionary rate variation among protein sites. *Nat. Rev. Genet.* **17**, 109-121 (2016).
7. Hughes, A.L. & Nei, M. Pattern of nucleotide substitution at major histocompatibility complex class I loci reveals overdominant selection. *Nature* **335**, 167-70 (1988).
8. Sawyer, S.L., Wu, L.I., Emerman, M. & Malik, H.S. Positive selection of primate TRIM5alpha identifies a critical species-specific retroviral restriction domain. *Proc Natl Acad Sci U S A* **102**, 2832-7 (2005).
9. Schott, R.K., Refvik, S.P., Hauser, F.E., Lopez-Fernandez, H. & Chang, B.S. Divergent positive selection in rhodopsin from lake and riverine cichlid fishes. *Mol Biol Evol* **31**, 1149-65 (2014).
10. Endo, T., Ikeo, K. & Gojobori, T. Large-scale search for genes on which positive selection may operate. *Mol Biol Evol* **13**, 685-90 (1996).
11. Kosiol, C. *et al.* Patterns of positive selection in six Mammalian genomes. *PLoS Genet* **4**, e1000144 (2008).
12. Eory, L., Halligan, D.L. & Keightley, P.D. Distributions of selectively constrained sites and deleterious mutation rates in the hominid and murid genomes. *Mol Biol Evol* **27**, 177-92 (2010).
13. Lindblad-Toh, K. *et al.* A high-resolution map of human evolutionary constraint using 29 mammals. *Nature* **478**, 476-82 (2011).
14. Roux, J. *et al.* Patterns of positive selection in seven ant genomes. *Mol Biol Evol* **31**, 1661-85 (2014).
15. Cicconardi, F., Marcatili, P., Arthofer, W., Schlick-Steiner, B.C. & Steiner, F.M. Positive diversifying selection is a pervasive adaptive force throughout the Drosophila radiation. *Mol Phylogenet Evol* **112**, 230-243 (2017).
16. Yang, Z., Nielsen, R. & Goldman, N. In defense of statistical methods for detecting positive selection. *Proc Natl Acad Sci U S A* **106**, E95; author reply E96 (2009).
17. Zhai, W., Nielsen, R., Goldman, N. & Yang, Z. Looking for Darwin in genomic sequences--validity and success of statistical methods. *Mol Biol Evol* **29**, 2889-93 (2012).
18. Laskowski, R.A. & Thornton, J.M. Understanding the molecular machinery of genetics through 3D structures. *Nat Rev Genet* **9**, 141-51 (2008).

19. Homburger, J.R. *et al.* Multidimensional structure-function relationships in human beta-cardiac myosin from population-scale genetic variation. *Proc Natl Acad Sci U S A* **113**, 6701-6 (2016).
20. Miller, M.L. *et al.* Pan-Cancer Analysis of Mutation Hotspots in Protein Domains. *Cell Syst* **1**, 197-209 (2015).
21. Kamburov, A. *et al.* Comprehensive assessment of cancer missense mutation clustering in protein structures. *Proc Natl Acad Sci U S A* **112**, E5486-95 (2015).
22. Niu, B. *et al.* Protein-structure-guided discovery of functional mutations across 19 cancer types. *Nat Genet* **48**, 827-37 (2016).
23. Araya, C.L. *et al.* Identification of significantly mutated regions across cancer types highlights a rich landscape of functional molecular alterations. *Nat Genet* **48**, 117-25 (2016).
24. Vilella, A.J. *et al.* EnsemblCompara GeneTrees: Complete, duplication-aware phylogenetic trees in vertebrates. *Genome Res* **19**, 327-35 (2009).
25. Mir, S. *et al.* PDBe: towards reusable data delivery infrastructure at protein data bank in Europe. *Nucleic Acids Res* **46**, D486-D492 (2018).
26. Dana, J.M. *et al.* SIFTS: updated Structure Integration with Function, Taxonomy and Sequences resource allows 40-fold increase in coverage of structure-based annotations for proteins. *Nucleic Acids Res* **47**, D482-D489 (2019).
27. Löytynoja, A. & Goldman, N. Phylogeny-aware gap placement prevents errors in sequence alignment and evolutionary analysis. *Science* **320**, 1632-1635 (2008).
28. Massingham, T. & Goldman, N. Detecting amino acid sites under positive selection and purifying selection. *Genetics* **169**, 1753-62 (2005).
29. Xie, T. *et al.* Crystal structure of the gamma-secretase component nicastrin. *Proc Natl Acad Sci U S A* **111**, 13349-54 (2014).
30. Enard, D., Cai, L., Gwennap, C. & Elife, D.A.P. Viruses are a dominant driver of protein adaptation in mammals. *cdn.elifesciences.org*.
31. Webb, A.E. *et al.* Adaptive Evolution as a Predictor of Species-Specific Innate Immune Response. *Mol Biol Evol* **32**, 1717-29 (2015).
32. Ebel, E.R., Telis, N., Venkataram, S., Petrov, D.A. & Enard, D. High rate of adaptation of mammalian proteins that interact with Plasmodium and related parasites. *PLOS Genetics* **13**, e1007023 (2017).
33. Sironi, M., Cagliani, R., Forni, D. & Clerici, M. Evolutionary insights into host-pathogen interactions from mammalian sequence data. *Nat Rev Genet* **16**, 224-36 (2015).
34. Demogines, A., Abraham, J., Choe, H., Farzan, M. & Sawyer, S.L. Dual host-virus arms races shape an essential housekeeping protein. *PLoS Biol.* **11**, e1001571 (2013).
35. Huntington, J.A., Read, R.J. & Carrell, R.W. Structure of a serpin-protease complex shows inhibition by deformation. *Nature* **407**, 923-926 (2000).
36. Ye, S. *et al.* The structure of a Michaelis serpin-protease complex. *Nat. Struct. Biol.* **8**, 979-983 (2001).
37. Kim, P.M., Korbel, J.O. & Gerstein, M.B. Positive selection at the protein network periphery: evaluation in terms of structural constraints and cellular context. *Proc. Natl. Acad. Sci. U. S. A.* **104**, 20274-20279 (2007).
38. Vidalino, L. *et al.* SERPINB3, apoptosis and autoimmunity. *Autoimmun Rev* **9**, 108-12 (2009).
39. Heit, C. *et al.* Update of the human and mouse SERPIN gene superfamily. *Hum. Genomics* **7**, 22 (2013).
40. Izuhara, K., Ohta, S., Kanaji, S., Shiraishi, H. & Arima, K. Recent progress in understanding the diversity of the human ov-serpin/clade B serpin family. *Cell Mol Life Sci* **65**, 2541-53 (2008).

41. Hughes, A.L., Ota, T. & Nei, M. Positive Darwinian selection promotes charge profile diversity in the antigen-binding cleft of class I major-histocompatibility-complex molecules. *Mol Biol Evol* **7**, 515-24 (1990).
42. Van Valen, L. *A new evolutionary law*, 1—30 (1973).
43. Lynch, T. & Price, A. The effect of cytochrome P450 metabolism on drug response, interactions, and adverse effects. *Am Fam Physician* **76**, 391-6 (2007).
44. Wilkinson, G.R. Drug metabolism and variability among patients in drug response. *N Engl J Med* **352**, 2211-21 (2005).
45. Penning, T.M. The aldo-keto reductases (AKRs): Overview. *Chem Biol Interact* **234**, 236-46 (2015).
46. Jin, Y. & Penning, T.M. Aldo-keto reductases and bioactivation/detoxication. *Annu Rev Pharmacol Toxicol* **47**, 263-92 (2007).
47. Bachur, N.R. Cytoplasmic aldo-keto reductases: a class of drug metabolizing enzymes. *Science* **193**, 595-7 (1976).
48. Barski, O.A., Tipparaju, S.M. & Bhatnagar, A. The aldo-keto reductase superfamily and its role in drug metabolism and detoxification. *Drug Metab. Rev.* **40**, 553-624 (2008).
49. Gloss, A.D. *et al.* Evolution in an ancient detoxification pathway is coupled with a transition to herbivory in the drosophilidae. *Mol. Biol. Evol* **31**, 2441-2456 (2014).
50. Lan, T., Wang, X.-R. & Zeng, Q.-Y. Structural and functional evolution of positively selected sites in pine glutathione S-transferase enzyme family. *J. Biol. Chem.* **288**, 24441-24451 (2013).
51. da Fonseca, R.R., Johnson, W.E., O'Brien, S.J., Vasconcelos, V. & Antunes, A. Molecular evolution and the role of oxidative stress in the expansion and functional diversification of cytosolic glutathione transferases. *BMC Evol. Biol.* **10**, 281 (2010).
52. Ivarsson, Y., Mackey, A.J., Edalat, M., Pearson, W.R. & Mannervik, B. Identification of Residues in Glutathione Transferase Capable of Driving Functional Diversification in Evolution: A novel approach to protein redesign. *J. Biol. Chem.* **278**, 8733-8738 (2003).
53. Wang, D. *et al.* Human carboxylesterases: a comprehensive review. *Acta Pharm Sin B* **8**, 699-712 (2018).
54. Bencharit, S., Morton, C.L., Xue, Y., Potter, P.M. & Redinbo, M.R. Structural basis of heroin and cocaine metabolism by a promiscuous human drug-processing enzyme. *Nat Struct Biol* **10**, 349-56 (2003).
55. Allali-Hassani, A. *et al.* Structural and chemical profiling of the human cytosolic sulfotransferases. *PLoS Biol* **5**, e97 (2007).
56. Gamage, N. *et al.* Human sulfotransferases and their role in chemical metabolism. *Toxicol Sci* **90**, 5-22 (2006).
57. Kerns, S.J. *et al.* The energy landscape of adenylate kinase during catalysis. *Nat. Struct. Mol. Biol.* **22**, 124-131 (2015).
58. Schrank, T.P., Wrabl, J.O. & Hilser, V.J. Conformational Heterogeneity Within the LID Domain Mediates Substrate Binding to Escherichia coli Adenylate Kinase: Function Follows Fluctuations. in *Topics in Current Chemistry* (eds. Klinman, J. & Schiffer, S.H.) 95-121 (Springer Berlin Heidelberg, 2013).
59. Schrank, T.P., Wrabl, J.O. & Hilser, V.J. Conformational heterogeneity within the LID domain mediates substrate binding to Escherichia coli adenylate kinase: function follows fluctuations. *Top Curr Chem* **337**, 95-121 (2013).
60. Jing, F. *et al.* Phylogenetic and experimental characterization of an acyl-ACP thioesterase family reveals significant diversity in enzymatic specificity and activity. *BMC Biochem.* **12**, 44 (2011).
61. Bai, X.C. *et al.* An atomic structure of human gamma-secretase. *Nature* **525**, 212-217 (2015).
62. Messier, W. & Stewart, C.B. Episodic adaptive evolution of primate lysozymes. *Nature* **385**, 151-4 (1997).

63. Zhang, J., Zhang, Y.P. & Rosenberg, H.F. Adaptive evolution of a duplicated pancreatic ribonuclease gene in a leaf-eating monkey. *Nat Genet* **30**, 411-5 (2002).
64. Furnham, N. *et al.* The Catalytic Site Atlas 2.0: cataloging catalytic sites and residues identified in enzymes. *Nucleic Acids Res* **42**, D485-9 (2014).
65. Jack, B.R., Meyer, A.G., Echave, J. & Wilke, C.O. Functional Sites Induce Long-Range Evolutionary Constraints in Enzymes. *PLoS Biol* **14**, e1002452 (2016).
66. Goldman, N., Thorne, J.L. & Jones, D.T. Assessing the impact of secondary structure and solvent accessibility on protein evolution. *Genetics* **149**, 445-58 (1998).
67. Bartlett, G.J., Porter, C.T., Borkakoti, N. & Thornton, J.M. Analysis of Catalytic Residues in Enzyme Active Sites. *J. Mol. Biol.* **324**, 105-121 (2002).
68. Ohno, S. *Evolution by gene duplication*, xv, 160 p. (Springer-Verlag, London, 1970).
69. Francino, M.P. An adaptive radiation model for the origin of new gene functions. *Nat Genet* **37**, 573-7 (2005).
70. Khersonsky, O., Roodveldt, C. & Tawfik, D.S. Enzyme promiscuity: evolutionary and mechanistic aspects. *Curr Opin Chem Biol* **10**, 498-508 (2006).
71. Schmidt, D.M. *et al.* Evolutionary potential of (beta/alpha)8-barrels: functional promiscuity produced by single substitutions in the enolase superfamily. *Biochemistry* **42**, 8387-93 (2003).
72. Rothman, S.C. & Kirsch, J.F. How does an enzyme evolved in vitro compare to naturally occurring homologs possessing the targeted function? Tyrosine aminotransferase from aspartate aminotransferase. *J Mol Biol* **327**, 593-608 (2003).
73. Hoffmeister, D., Yang, J., Liu, L. & Thorson, J.S. Creation of the first anomeric D/L-sugar kinase by means of directed evolution. *Proc Natl Acad Sci U S A* **100**, 13184-9 (2003).
74. Aharoni, A. *et al.* The 'evolvability' of promiscuous protein functions. *Nat Genet* **37**, 73-6 (2005).
75. Zhou, Y., Mkrtchian, S., Kumondai, M., Hiratsuka, M. & Lauschke, V.M. An optimized prediction framework to assess the functional impact of pharmacogenetic variants. *Pharmacogenomics J* **19**, 115-126 (2019).
76. Bloom, J.D. Identification of positive selection in genes is greatly improved by using experimentally informed site-specific models. *Biol. Direct* **12**, 1 (2017).
77. Parmley, J.L., Chamary, J.V. & Hurst, L.D. Evidence for purifying selection against synonymous mutations in mammalian exonic splicing enhancers. *Mol Biol Evol* **23**, 301-9 (2006).
78. Macossay-Castillo, M., Kosol, S., Tompa, P. & Pancsa, R. Synonymous constraint elements show a tendency to encode intrinsically disordered protein segments. *PLoS Comput Biol* **10**, e1003607 (2014).
79. Savisaar, R. & Hurst, L.D. Both Maintenance and Avoidance of RNA-Binding Protein Interactions Constrain Coding Sequence Evolution. *Mol Biol Evol* **34**, 1110-1126 (2017).
80. Davydov, II, Salamin, N. & Robinson-Rechavi, M. Large-Scale Comparative Analysis of Codon Models Accounting for Protein and Nucleotide Selection. *Mol Biol Evol* (2019).
81. Schneider, A. *et al.* Estimates of positive Darwinian selection are inflated by errors in sequencing, annotation, and alignment. *Genome Biol Evol* **1**, 114-8 (2009).
82. Jordan, G. & Goldman, N. The effects of alignment error and alignment filtering on the sitewise detection of positive selection. *Mol Biol Evol* **29**, 1125-39 (2012).
83. Perron, U., Moal, I., Thorne, J. & Goldman, N. Probabilistic Models for the Study of Protein Evolution. *In D. Balding, I. Moltke, and J. Marioni, editors, Handbook of Statistical Genetics. Wiley-Interscience, 4th edition.* (In Press).

84. Perron, U., Kozlov, A.M., Stamatakis, A., Goldman, N. & Moal, I.H. Modelling structural constraints on protein evolution via side-chain conformational states. *Mol. Biol. Evol.* (In Press).

462

463 ## Methods

464 ### Genomic data

465 Coding sequences for mammalian genomes were downloaded from Ensembl [85], version 78.
466 Non-eutherian genomes (platypus, gray short-tailed opossum, wallaby and Tasmanian devil)
467 were excluded. Coding sequences for principal isoforms were used. Incomplete and stop
468 codons at ends of sequences were removed.

469 ### Phylogenetic data

470 The Compara database [86] provides gene trees for species stored in Ensembl. The Compara
471 pipeline generates trees containing up to 750 related genes which frequently results in multiple
472 paralogs being included in the same tree. Bearing in mind that selective constraint can be
473 estimated more accurately if more sequences are included, but that including more paralogs
474 can result in averaging over genes which may be under different constraints, we designed a
475 tree-splitting scheme to enable single-gene analysis. As we aimed to maximise the number of
476 orthologous sequences included in each alignment while minimising the number of paralogous
477 sequences, we quantified these criteria in different possible subtrees by calculating the
478 percentage of all species included (taxonomic coverage) and the total number of additional
479 genes for each species beyond the first gene per species (permitting calculation of the paralog
480 fraction). We required a taxonomic coverage of at least 60% and wished to minimise the
481 paralog fraction. To achieve this, starting from each human protein, the tree is traversed
482 towards the root until the desired taxonomic coverage was achieved. Then, the tree is
483 traversed further but only if this does not increase the paralog fraction. The final node of this
484 traversal process and all its descendant nodes then become a tree used for further analysis.

485 **Sequence alignment**

486 Compara gene trees are reconstructed using principal isoforms and the same sequences were
487 used for alignment. The PRANK aligner [27] has been show to limit the number of false positive
488 identifications of positive selection compared to other commonly used aligners [82,87,88]. PRANK
489 was run in codon mode on sets of sequences corresponding to each Compara-derived tree
490 and with these trees used as guide trees.

491 **Detecting positive selection**

492 SLR [28] was used to obtain sitewise estimates of ω within each alignment, using tree topologies
493 from Ensembl Compara and allowing branch lengths to be optimised by SLR. SLR implements
494 a statistical test for positive selection based on the rates of fixation of nonsynonymous and
495 synonymous mutations (ω, or dN/dS). This measure is derived from neutral theory [89,90], which
496 provides a general framework for studying selective effects and allows for explicitly identifying
497 genomic regions that evolve under positive selection. If mutations that arise are deleterious,
498 they will undergo purifying selection and will be purged from a population, resulting in a low
499 observed evolutionary rate. Conversely, if mutations result in beneficial changes, they will be
500 rapidly driven to fixation. The ratio of fixation probabilities of nonsynonymous and synonymous
501 substitutions can thus be used to estimate the selective constraint acting on the protein level:
502 $\omega \approx 1$ indicates neutral evolution; $\omega < 1$ purifying selection; and $\omega > 1$ positive selection [91].
503 SLR implements the Goldman-Yang codon site model [92] similar to that in PAML [3]. The main
504 difference between SLR and PAML is that SLR makes no assumption about the distribution of
505 ω values over the sites of the alignment. SLR first estimates parameters of the phylogenetic
506 model for the entire alignment and then performs a likelihood ratio test between the optimal
507 ω and $\omega = 1$ for each site. *P*-values reported by SLR associated with each structure-mapped
508 site (see below) were then corrected for multiple testing using the Benjamini-Hochberg FDR
509 method [93].

510 **Structural data**

511 PDB structures matching human proteins in the sequence dataset were downloaded from
512 PDBe [25]. Structures covering fewer than 100 residues were excluded, and in cases where
513 more than one structure was available the one with the highest sequence similarity to the
514 protein sequence was chosen. In rare cases where more than one human protein with a
515 structure was present for an alignment, one was retained at random. Individual residues were
516 then mapped using the SIFTS database [26]. SIFTS provides a mapping between PDB [25] and
517 UniProt [94] sequences and, as the UniProt protein sequences can vary from those in Ensembl,
518 we performed an additional mapping step by constructing pairwise alignments between
519 UniProt and Ensembl sequences, resulting in a sitewise mapping between Ensembl and PDB
520 residues. The pairwise alignments were calculated using the Biopython [95] implementation of
521 the Smith-Waterman algorithm [96], using the scoring of 1 for matching characters and 0
522 otherwise, and gap opening and extension penalties of -10 and -0.5 respectively.

523 **Clustering of positively selected sites**

524 The degree of clustering of the positively selected sites within each protein structure was
525 assessed using the CLUMPS algorithm [21]. In CLUMPS, the degree of clustering for a set of
526 residues of interest is quantified by the sum of pairwise distances in 3D space. In contrast to
527 the original implementation, we used equal weights for all sites when calculating the pairwise
528 distances. For each set of residues, we then performed 100,000 Monte Carlo simulations
529 permuting the placement of sites by randomly selecting positions from the PDB chain, in order
530 to determine statistical significance of observed patterns. *P*-values resulting from this analysis
531 were then corrected for multiple comparisons using the Benjamini-Hochberg FDR method [93].

532 Statistical analyses were performed in the R environment [97].

533 **References**

85. Cunningham, F. *et al.* Ensembl 2019. *Nucleic Acids Res* **47**, D745-D751 (2019).
86. Herrero, J. *et al.* Ensembl comparative genomics resources. *Database* **2016**(2016).

87. Fletcher, W. & Yang, Z. The effect of insertions, deletions, and alignment errors on the branch-site test of positive selection. *Mol Biol Evol* **27**, 2257-67 (2010).
88. Markova-Raina, P. & Petrov, D. High sensitivity to aligner and high rate of false positives in the estimates of positive selection in the 12 Drosophila genomes. *Genome Res* **21**, 863-74 (2011).
89. Kimura, M. Evolutionary rate at the molecular level. *Nature* **217**, 624-6 (1968).
90. Kimura, M. On the probability of fixation of mutant genes in a population. *Genetics* **47**, 713-9 (1962).
91. Nei, M. & Gojobori, T. Simple methods for estimating the numbers of synonymous and nonsynonymous nucleotide substitutions. *Mol Biol Evol* **3**, 418-26 (1986).
92. Goldman, N. & Yang, Z. A codon-based model of nucleotide substitution for protein-coding DNA sequences. *Mol Biol Evol* **11**, 725-36 (1994).
93. Benjamini, Y. & Hochberg, Y. Controlling the False Discovery Rate: A Practical and Powerful Approach to Multiple Testing. *Journal of the Royal Statistical Society. Series B (Methodological)* **57**, 289-300 (1995).
94. UniProt Consortium, T. UniProt: the universal protein knowledgebase. *Nucleic Acids Res* **46**, 2699 (2018).
95. Cock, P.J. *et al.* Biopython: freely available Python tools for computational molecular biology and bioinformatics. *Bioinformatics* **25**, 1422-3 (2009).
96. Smith, T.F. & Waterman, M.S. Identification of common molecular subsequences. *J Mol Biol* **147**, 195-7 (1981).
97. Development Core Team, R. R Core Team. R: A Language and Environment for Statistical Computing 2014. (2013).

534 **Tables**

Gene symbol	Gene name	Protein length	PDB	PDB sites	Substrate/relevant ligand in PDB	Number of pos. sel. sites[1]
Immune-related proteins						
HLA-DRBI	major histocompatibility complex, class II, DR beta 1	266	1aqd	187	endogenous peptide	16/19/21/25
FCN2	Ficolin 2	313	2j3f	217	N-acetyl-D-galactosamine	6/9/10/13
SERPINB3	Serpin B3	390	4zk0	367	-	24/26/31/42
TLR4	toll-like receptor 4	839	4g8a	601	LPS, LP4	51/61/80/119
CD1A	CD1a molecule	327	1onq	271	sulfatide self-antigen	40/44/50/64
C5	Complement component 5	1676	3cu7	1625	-	28/37/53/89
C8A	Complement component 8α	584	3ojy	478	-	16/20/27/34
SIGLEC5	Sialic acid binding Ig-like lectin 5	551	2zg1	208	sialic acid	24/32/38/43
TFRC	transferrin receptor 1	760	3s9l	638	-	17/19/24/40
Metabolic enzymes						
CYP2C9	Cytochrome P450, family 2, member C9	490	1r9o	453	flurbiprofen	29/30/35/40
CYP2D6	Cytochrome P450, family 2, member D6	497	2f9q	454	-	6/8/10/14
CYP3A4	Cytochrome P450, family 3, member A4	503	3tjs	449	desthiazolylmethyloxycarbonyl ritonavir	22/27/33/41
AKR1B10	Aldo-keto reductase family 1, member B10	316	1zua	316	tolrestat	13/18/19/23
AKR1C4	Aldo-keto reductase family 1, member C4	323	2fvl	323	-	19/21/23/26
SULT2A1	Sulfotransferase family 2A member 1	285	3f3y	282	lithocholic acid	15/18/22/32
CES1	Carboxylesterase 1	568	1mx1	532	tacrine	12/16/19/31
GSTA3	Glutathione S-transferase alpha 3	222	1tdi	218	glutathione	11/13/16/20
OLAH	Oleoyl-ACP hydrolase	318	4xjv	216	-	8/12/18/24
AK5	Adenylate kinase 5	562	2bwj	195	AMP	3/3/3/3
NCSTN	Nicastrin	709	5a63	665	phosphocholine	7/8/11/18

535 **Table 1.** Proteins with clusters of positively selected sites. Protein length refers to human orthologs.
536 [1]The number of positively selected sites is given at FDR thresholds of 0.05, 0.1, 0.2 and 0.5, respectively.